Supplementary Information

Regulating structural dimensionality and emission colors by organic conjugation between Sm^{III} at fixed distance

Hai-Bing Xu, Jie Wang, Xue-Li Chen, Xu Peng, Kang-Tai Xiong, Dao-Bin Guan, Jian-Guo Deng, Zhi-Hua Deng, Mohamedally Kurmoo, and Ming-Hua Zeng

Table of Sections

I. Investigation on dinuclear lanthanide with diphenylphosphine oxide as bridging ligand

Table S1 Lanthanide of diphenylphosphine oxide of similar length but different conjugation as bridging ligand

Complexes	Ln-Ln distance	Ref.
L1		
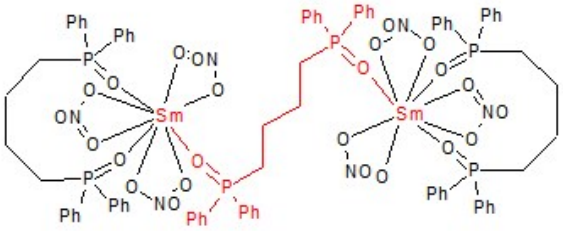	10.02	*Polyhedron,* **2006**, *25*, 809
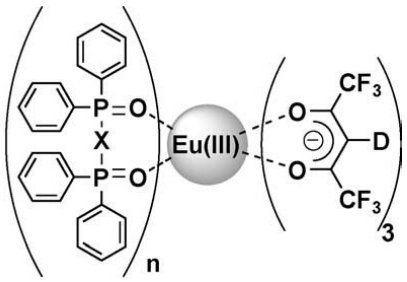		*J. Alloys and Compd.,* **2006**, *408,* 771-775
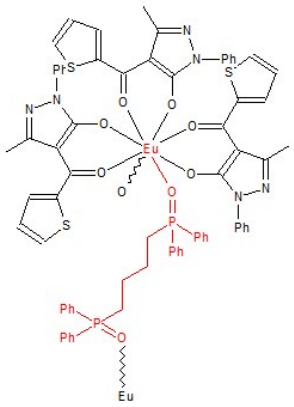	10.13	*Inorg. Chim. Acta.,* **2010**, *363*, 4083
L2		

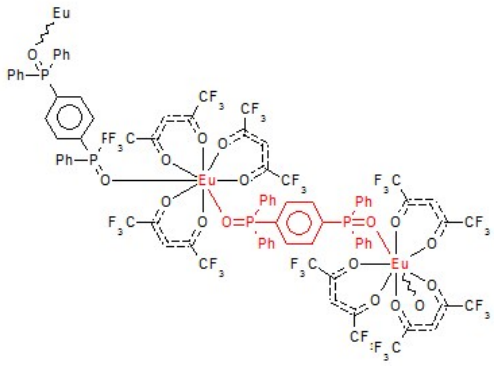	10.38	*ChemPlusChem.*, **2012**, *77*, 277
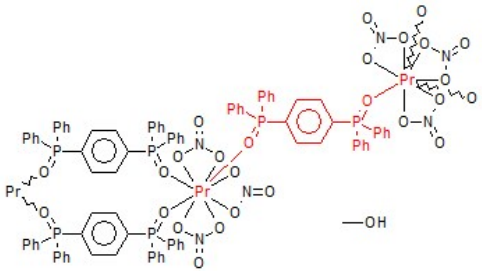	9.95 11.55	*Polyhedron*, **2011**,*30*, 1620
L3		
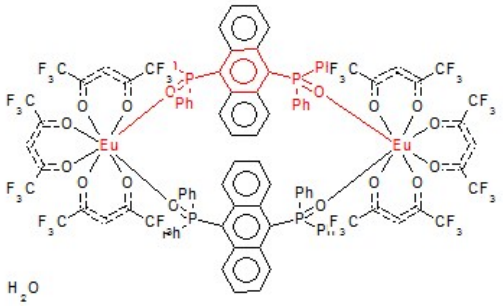	11.395	*Scientific Reports.*, **2013**, *3*, 2199

II. Crystal structures

Table S2. Crystallographic Data of 1, 2 and 3•0.5C_6H_{14}.

	1	**2**	**3·0.5C_6H_{14}**
Empirical formula	$C_{43}H_{31}F_{18}O_8P_2Sm$	$C_{57}H_{38}F_{15}O_9P_3Sm$	$C_{56}H_{38}F_{18}O_8P_2Sm$
Formula weight	1229.97	1395.13	1393.15
Space group	$P\ \bar{1}$	$P\ \bar{1}$	*C 2/c*
a (Å)	12.480(3)	13.7096(3)	29.2306(4)
b (Å)	13.211(3)	14.2767(3)	22.6434(3)
c (Å)	17.305(4)	16.7940(2)	20.0087(3)
α, deg	79.82(3)	95.4480(10)	90.00
β, deg	76.00(3)	93.0410(10)	123.4240(10)
γ, deg	66.05(3)	107.903(2)	90.00
V (Å^3)	2520.1(9)	3102.00(11)	11053.1(3)
Z	2	2	8
D_c (g cm^{-3})	1.621	1.494	1.674
□ (mm^{-1})	1.343	1.120	1.236
Radiation (*λ*□ Å)	0.71073	0.71073	0.71073
Temp (K)	293(2)	293(2)	143(2)
Independent Reflections	8723	10880	9710
Observed reflections with $I > 2\sigma(I)$	7033	8745	7932
R(int)	0.0466	0.0335	0.0315
$R1(F_o)$[a]	0.051	0.0580	0.0340
$wR2(F_o^2)$[b]	0.1303	0.1637	0.0804
GOF	1.038	1.058	1.040

[a] $R_1 = \Sigma||F_o|-|F_c||/\Sigma|F_o|$, [b] $wR_2 = [\Sigma w(F_o^2-F_c^2)^2 / \Sigma w(F_o^2)^2]^{1/2}$

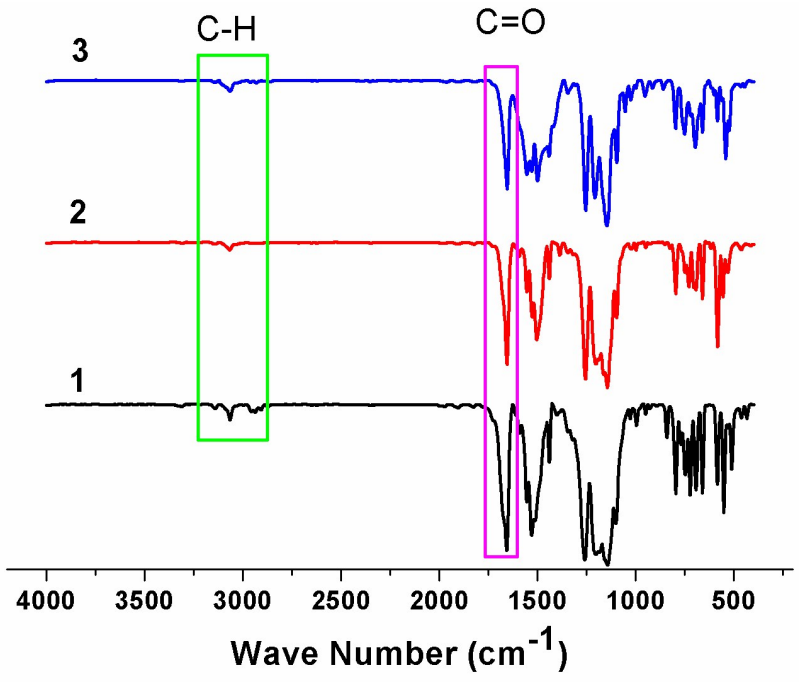

Figure S1. FTIR spectra of **1-3** with highlighting the principal assignations

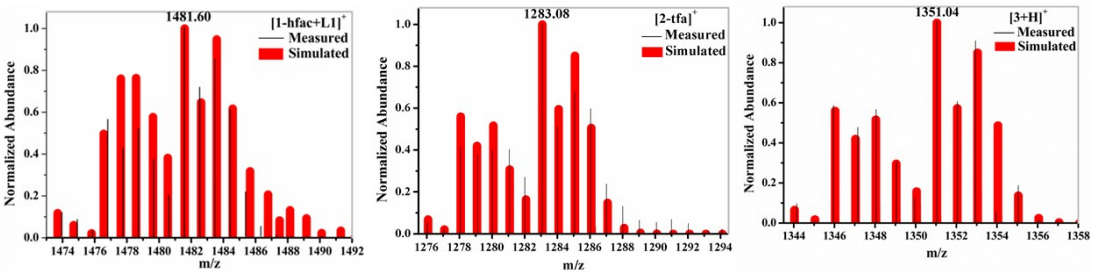

Figure S2. Positive ion ESI-MS of **1-3** in CH_2Cl_2-CH_3OH under the temperature of 275 ℃ (hfac$^-$ = hexafluoroacetylacetonato; tfa$^-$ = CF_3COO^-)

The PXRD patterns of **1-3** match the simulated ones using the single crystal structure data (Figures S3). These results confirm the single-phase nature of the bulk. The thermal stability of the compounds was investigated at a heating rate of 20 °C/min over the temperature range from 30 to 800 °C in flowing N_2. TGA (Figure S4) reveal that **1** and **2** are stable before 300 °C. As for **3**, it undergoes weight losses of 3.70 % below 100 °C, corresponding to the departure of $0.5C_6H_{14}$ and $0.5H_2O$ (calc. 3.73%). Then it is gradually decomposed with increasing temperature, indicating their stability up to 300 °C.

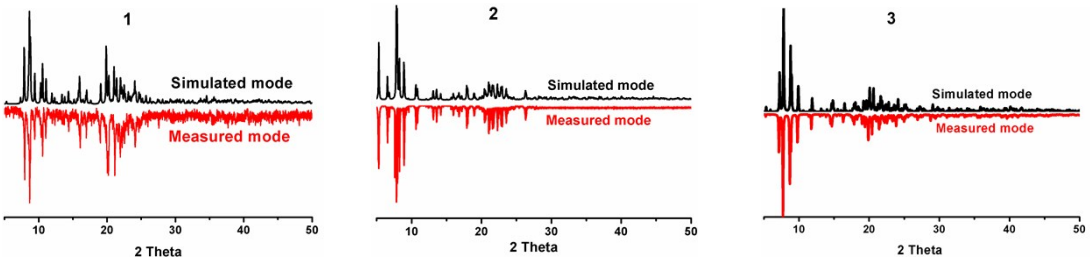

Figure S3. Comparison between the experimental and simulated diffraction patterns of **1-3**

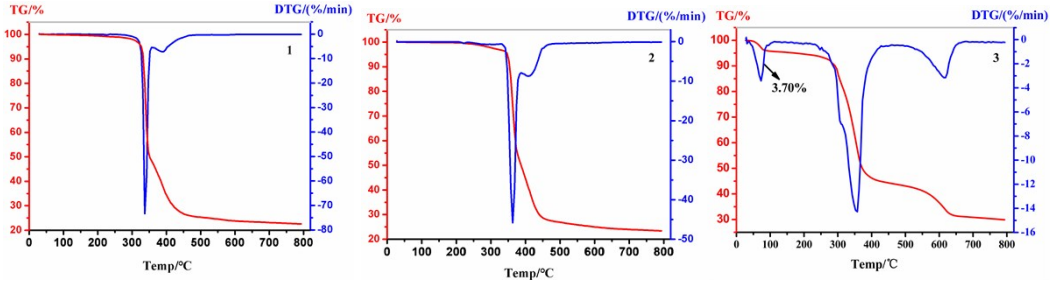

Figure S4. The TG curves of **1-3** over the temperature range of 30-800 °C with a heating rate of 20 °C/min in flowing N_2.

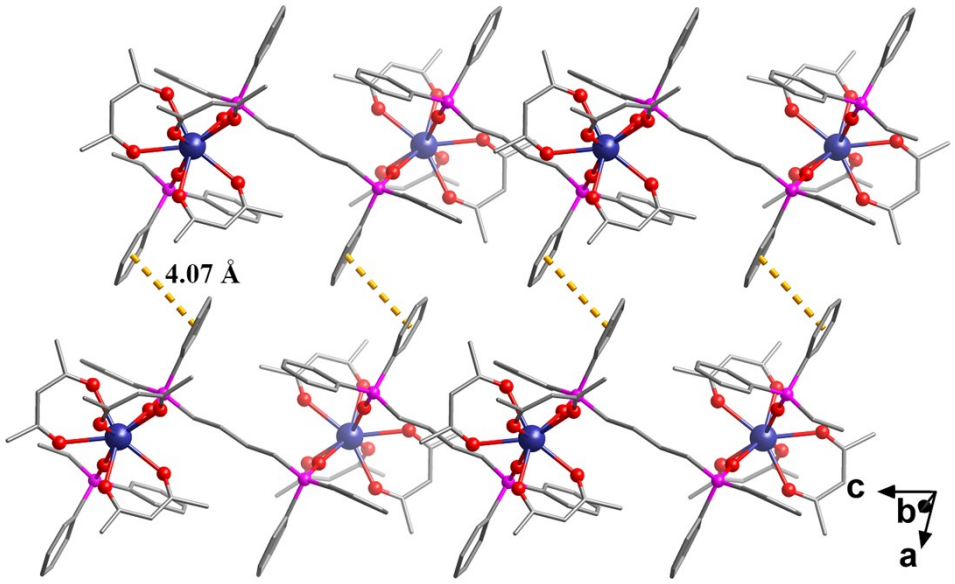

Figure S5. The packing in **1**, showing the intermolecular $\pi\cdots\pi$ stacking interaction.

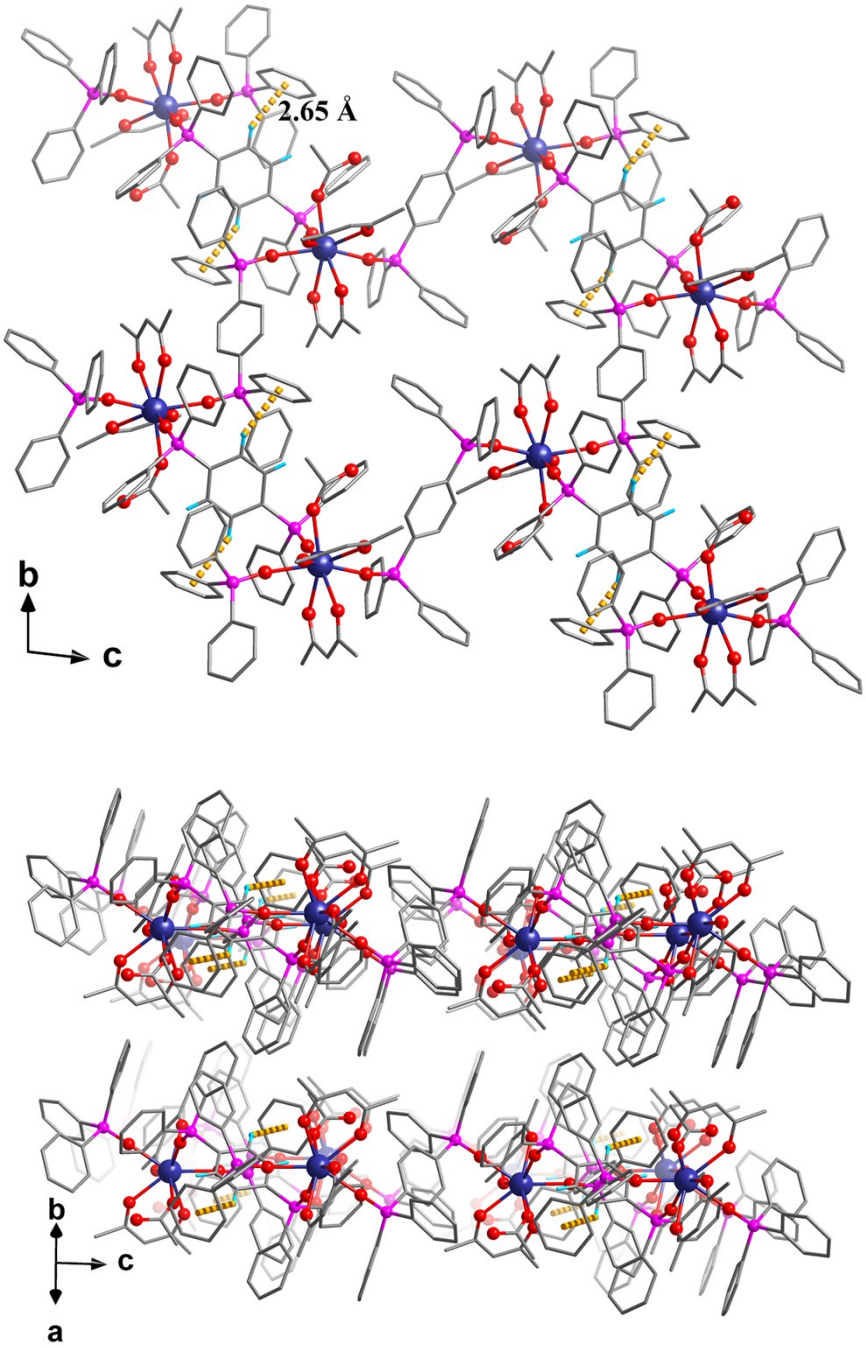

Figure S6. The 2D layer of **2**, showing intralayer C-H···π stacking interactions between layers.

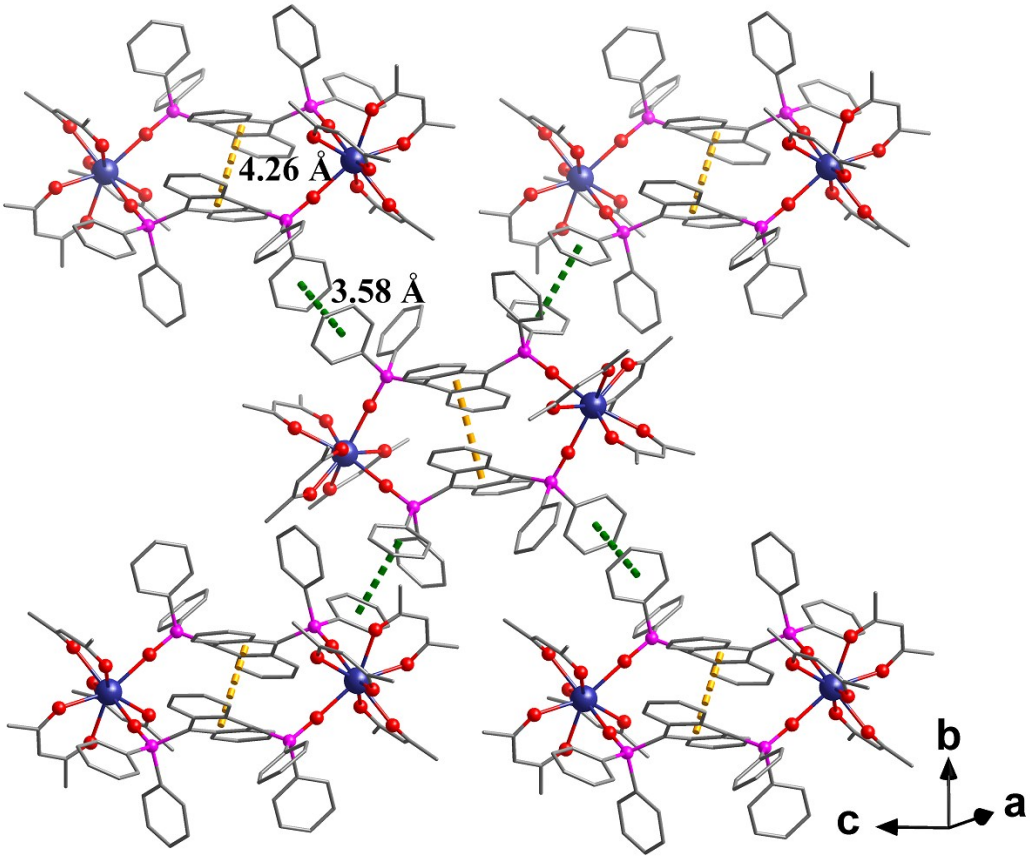

Figure S7. The packing of **3**, showing intramolecular $\pi\cdots\pi$ stacking interaction between **L3.**

III. UV-vis absorption spectra

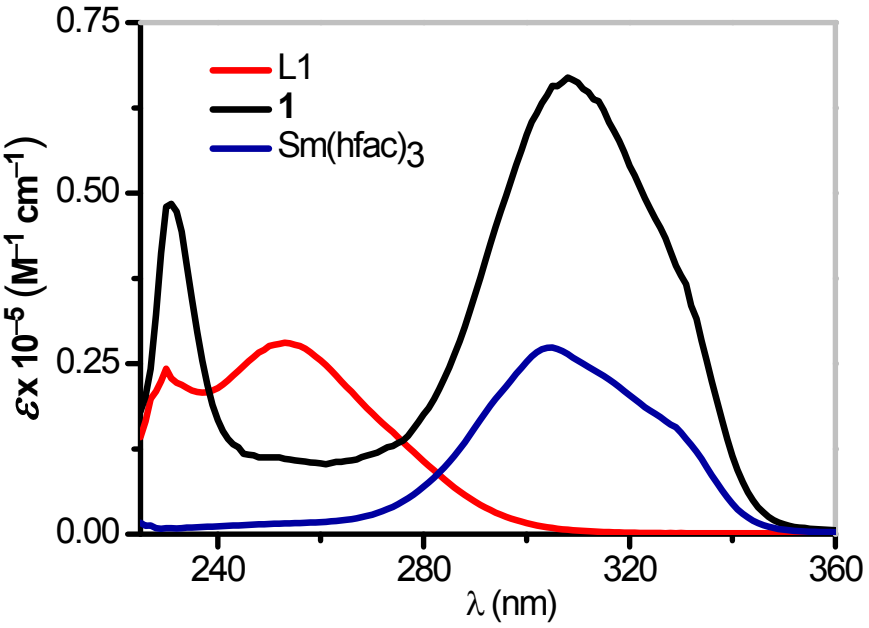

Figure S8. UV-vis absorption spectra of **L1**, **Sm(hfac)$_3$·2H$_2$O** and **1** in dichloromethane at ambient temperature.

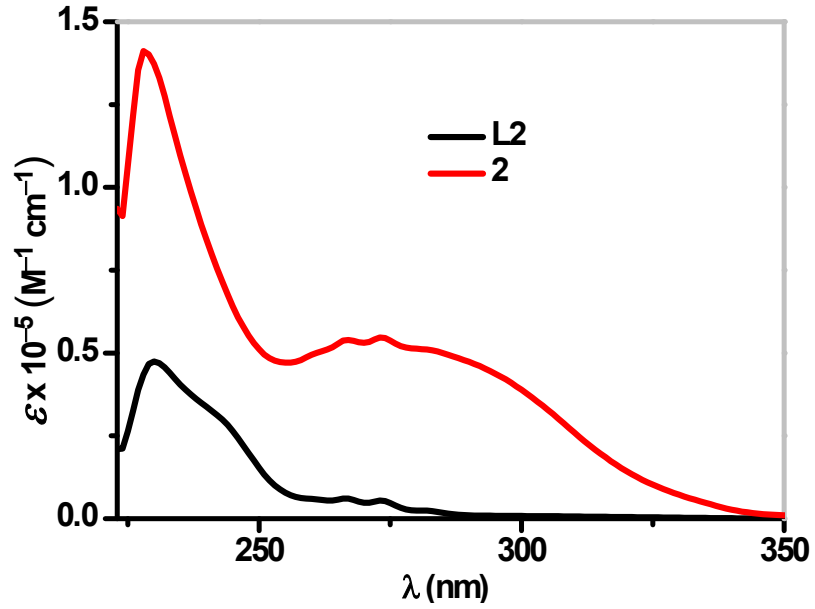

Figure S9. UV-vis absorption spectra of **L2** and **2** in dichloromethane at ambient temperature.

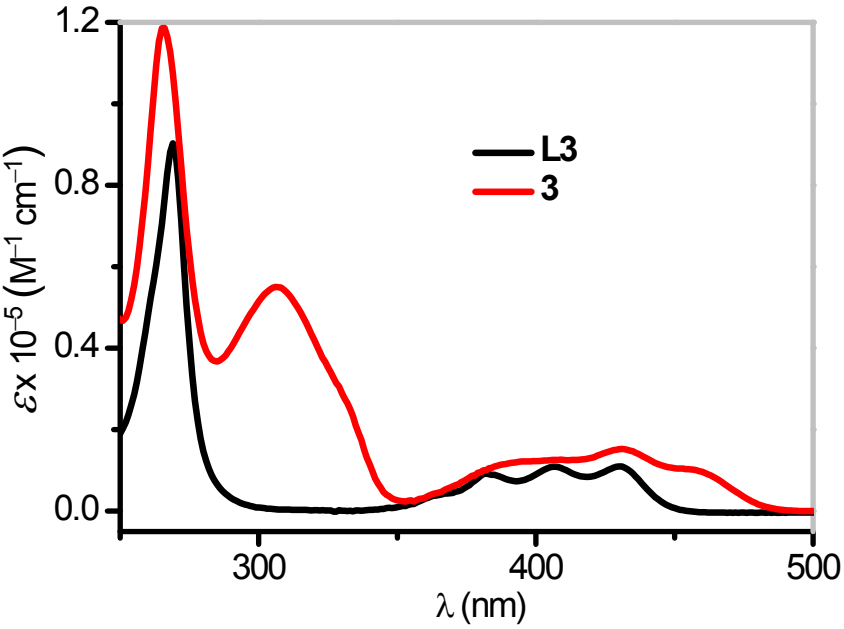

Figure S10. UV-vis absorption spectra of **L3** (black) and **3** (red) in dichloromethane at ambient temperature.

IV. Fluorescence spectra

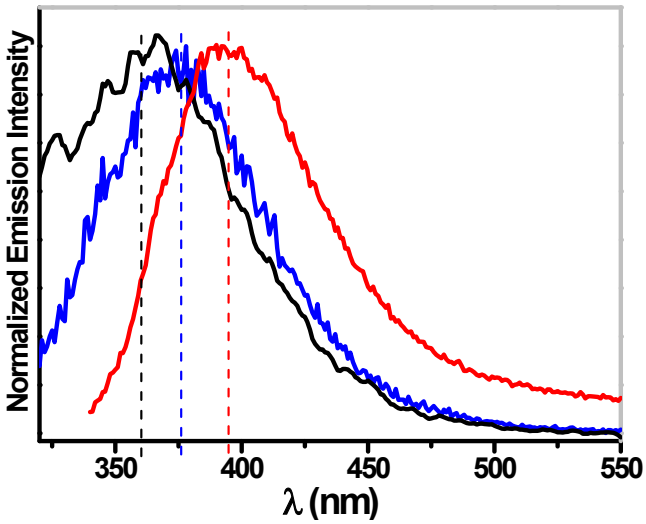

Figure S11. Normalized emission spectra (λ_{ex}= 282 nm) of **L2** of concentration 1×10^{-5} M (black) and 1×10^{-3} M (blue) in dichloromethane together with solid state (red) at ambient condition, showing redshift by aggregation effect.

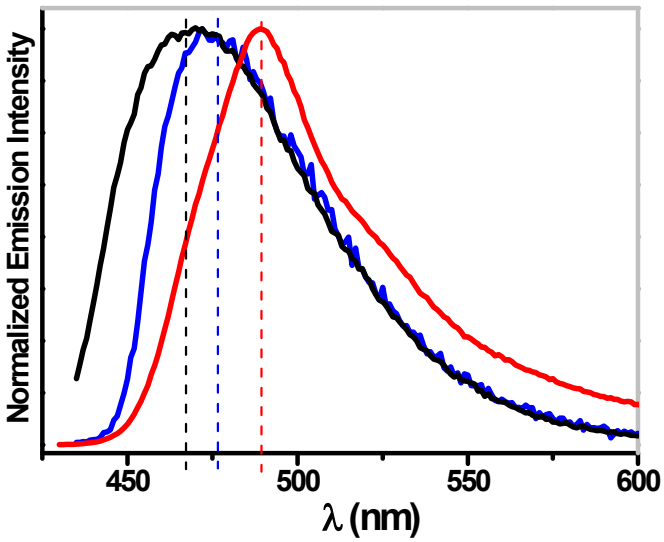

Figure S12. Normalized emission spectra (λ_{ex}= 384 nm) of **L3** of concentration 1×10^{-5} M (black) and 1×10^{-3} M (blue) in dichloromethane together with solid state (red) at ambient temperature, showing redshift by aggregation effect.

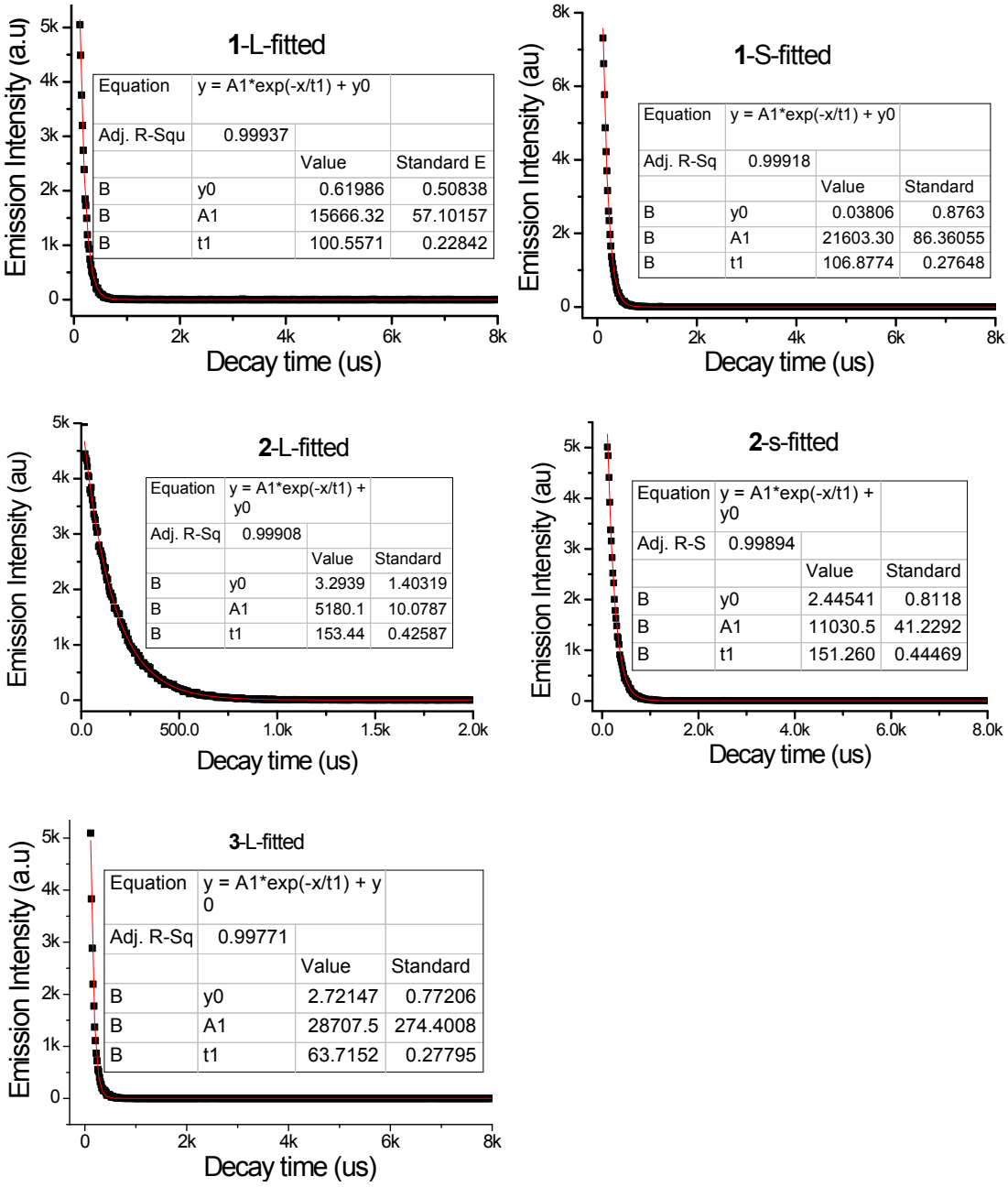

Figure S13. Lifetime decay curves of **1-3** in solid state (right) and solution (left) at 298 K.

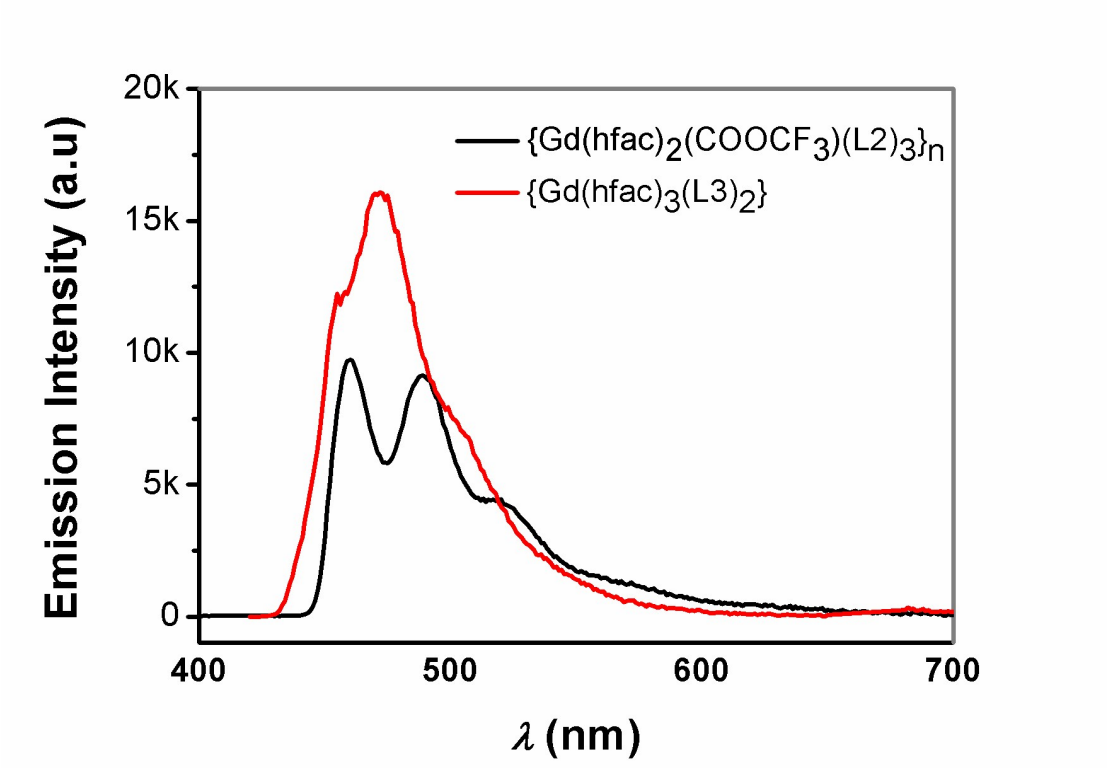

Figure S14. Emission spectra of $\{Gd(hfac)_2(CF_3COO)(\mathbf{L2})_3\}_\infty$ (λ_{ex} =330 nm) and $\{Gd(hfac)_3(\mathbf{L3})\}_2$ (λ_{ex} = 380 nm) with the concentration of 1.5×10^{-5} M in methane solutions at 77K.

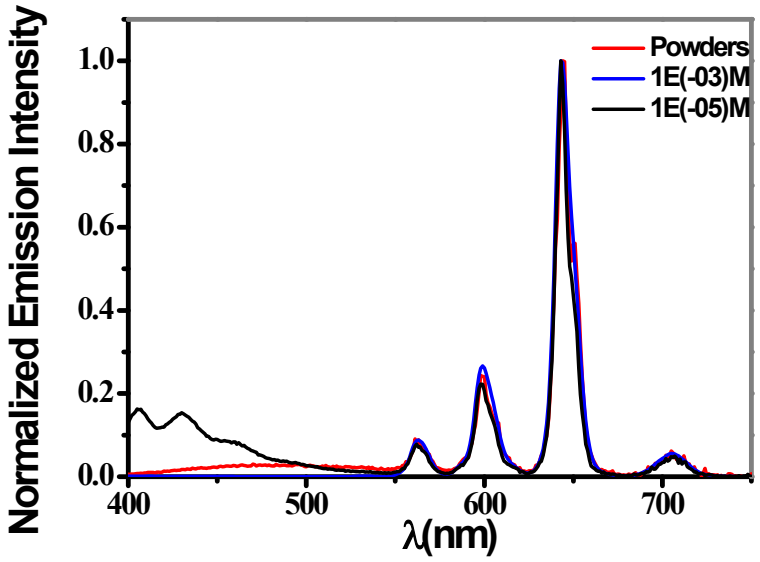

Figure S15. Emission spectra (λ_{ex} = 330 nm) of **1** in dichloromethane of concentration of 1×10^{-5} M (black), 1×10^{-3} M (blue) and in solid state (red) at ambient temperature.

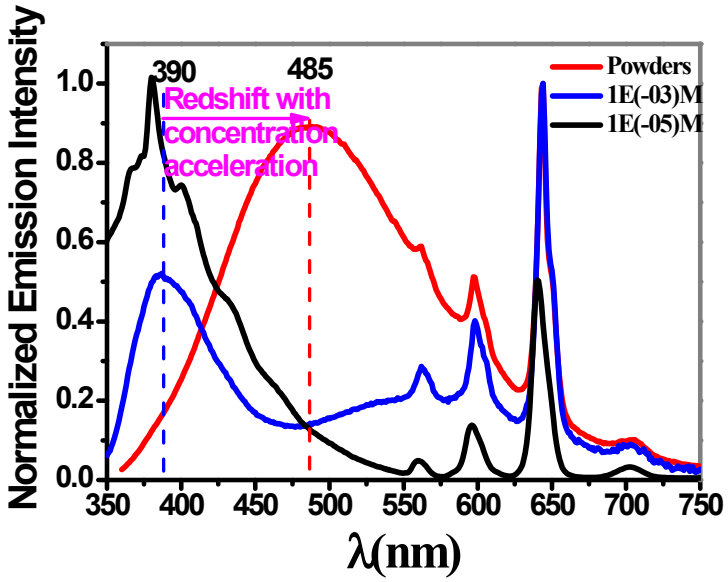

Figure S16. Emission spectra (λ_{ex} = 330 nm) of **2** in dichloromethane of concentration of 1×10^{-5} M (black), 1×10^{-3} M (blue) and in solid state (red) at ambient temperature, **L2**-based emission in **2** exhibiting redshift.